

Observations on High Reynolds Number Turbulent Boundary Layer Measurements

S. Hafez¹, M.S. Chong¹, I. Marusic² and M.B. Jones³

¹Department of Mechanical & Manufacturing Engineering
The University of Melbourne, VIC, 3010 AUSTRALIA

²Department of Aerospace Engineering & Mechanics
University of Minnesota, Minneapolis, MN 55455, USA

³School of Mathematical Sciences
Queensland University of Technology - Gardens Point Campus
GPO Box 2434

Abstract

An experimental study that examines spatial resolution effects on the measured streamwise velocity component is presented. Normal hot-wire measurements for mean flow velocity profiles, streamwise turbulence intensity profiles in addition to their respective spectra at different levels within the turbulent boundary layers will be presented. Measurements were carried out at Reynolds number based on momentum thickness, $R_\theta = 20,000$. Matching the same Reynolds number of the flows is achieved by varying the measuring station and consequently the reference freestream velocity. Wires of non-dimensional lengths l^+ , ranging from 11–54, were used. These measurements show that attenuation in hot-wire signals for long wires extend not only deep within the boundary layer, but also to the low wavenumber part of the spectra. It is conjectured that wires with the same l^+ , will be prone to further attenuation due to the increase of end conduction loss with increasing freestream velocity.

Introduction

Hot-wire anemometry is one of the most commonly used measuring techniques for turbulence research. The measured signal is the spatial average of the signature of eddies moving past the wire. Eddies of smaller size than the wire length will not correctly contribute to the higher order statistics of the flow. The inability to resolve these small eddies, commonly known as spatial resolution effects, is relevant to turbulence measurements for flows at high Reynolds number and for measurements close to solid boundaries. This is a direct result of the reduction in the size of the small scale viscous dissipative eddies and the anisotropy of the flow.

The limiting size of eddies in turbulent flows is the Kolmogoroff length scale, η . Within the turbulent wall region of wall-bounded flows it can be estimated as $\eta = (\nu^3 \kappa z / U_\tau^3)^{1/4}$ (see Perry *et al.* [8]). Here z is the wall-normal distance, ν is the kinematic viscosity, κ is the Karman constant and U_τ is the friction velocity. Ligrani & Bradshaw [6] carried out extensive normal hot-wire measurements in a boundary layer flow with $R_\theta = 2620$. Near-wall measurements with sub-miniature normal hot-wire sensors revealed that a wire of length, $l^+ = l / (\nu / U_\tau) < 20-25$ is sufficient to yield 'true' turbulence intensity measurements to within 4%. They suggest that wires with an aspect ratio (length/diameter) of approximately 200 will produce a uniform temperature along the wire length that will reduce the end conduction effect and improve the temporal resolution of the wire. These limits are commonly used as a guide for selecting sensors for turbulence measurements.

The effect of the sensor size in turbulence measurements has been recently investigated by Hites [5]. Normal hot-wire

measurements were carried out along a cylindrical model with a diameter of 45.7cm and length of 900cm. Different wires with diameters ranging from 0.6 μm –3.8 μm were tested at two measuring stations. The first measuring station was located at 184cm from the tripping device. At this station R_θ varied from 4100–9720, corresponding to viscous length, ν / U_τ , of 26 μm –11 μm . The second measuring station was 733cm from the tripping device with freestream velocity of 28.6m/s, $R_\theta = 19,300$ and $\nu / U_\tau = 17\mu\text{m}$. Turbulence intensity profiles measured with two different wires, $l^+ = 6$ and 31, which should not collapse due to the large difference in l^+ , showed complete collapse. This implies that a wire length of $l^+ = 30$ is sufficiently small to resolve turbulent flows which is not consistent with the findings of Ligrani & Bradshaw [6].

A new wind tunnel has recently been constructed at the University of Melbourne to study turbulent boundary layer flow at high Reynolds number. Attention was given at the design stage to produce flows that can be measured and resolved adequately. The wind tunnel was built to be "big and slow" and the high Reynolds number of the flow which can be achieved, is the outcome of having a long development length and relatively low freestream velocity.

Mean flow measurements by Hafez *et al.* [4], have shown mean flow characteristics to be dependent only on R_θ . Also, the velocity defect plots showed self-similar profiles for $R_\theta > 20,000$. This behaviour is consistent with the calculated Coles' wake factor, which approaches an asymptotic value for large R_θ .

The main objective of this study is to produce detailed normal hot-wire measurements for the streamwise velocity component at high Reynolds number. These measurements will include mean flow velocity profiles, turbulence intensity profiles for the streamwise velocity component and their respective spectra. Carrying out these measurements at the same Reynolds number, with controlled variation of spatial resolution, will help explain the observed discrepancy in recent studies and provide a framework for further hot-wire measurements. It can also be used to check recently proposed similarity laws for the mean flow, Reynolds stresses and spectra.

Apparatus and Techniques

The test facility is an open return blower wind tunnel with a 27m working length and a 2m x 1m cross section. Measurements were carried out for boundary layers developing on the tunnel floor, which is covered by aluminium plates of 6m x 2m and 6mm in thickness. The measured surface roughness of these plates is 1.5 μm (rms). All boundary layers developing along the inner surface of the nozzle were tripped using grade 40 sandpaper sheets, of 115mm width, glued on the nozzle inner surface, 750mm upstream from the exit. Figure 1 shows the main features of the test facility.

Measurements were limited to three reference unit Reynolds numbers of $U_\infty/\nu = 6.48 \times 10^5$, 1.03×10^6 and $1.59 \times 10^6/m$, where U_∞ is the reference free-stream velocity. They corresponding to nominal reference freestream velocity of 10m/s, 16m/s and 24m/s, respectively. Ambient flow conditions were measured using a calibrated thermocouple and an electronic barometer.

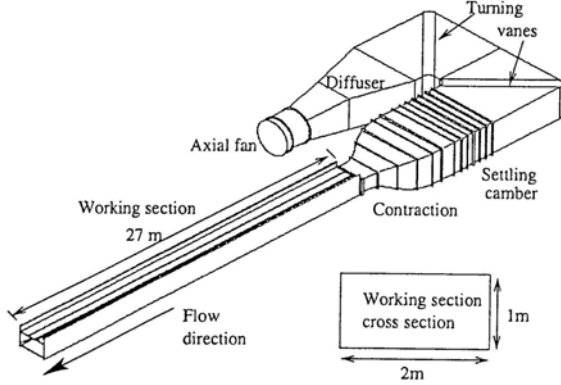


Figure 1: Isometric view of wind tunnel.

A nominally zero pressure gradient was maintained along the working section. The pressure coefficient C_p , which can be written as

$$C_p = 1 - \left(\frac{U_1}{U_\infty} \right)^2, \quad (1)$$

is kept constant along the entire 26m measuring section of the tunnel to within $\pm 1\%$, or better, for the velocity range covered in this study.

The normal single sensor (DANTEC 55P05) is used with a constant temperature anemometer system (AN-1003 from AA lab systems). Wollaston wires are soldered to the probe and etched to give a platinum filament with core diameters of $5.0\mu\text{m}$ and $2.5\mu\text{m}$, with active lengths of approximately 0.9mm and 0.55mm respectively. A static calibration technique, with a third order polynomial curve fit, is used to convert the measured anemometer output voltage into velocity. The normal hot-wire is calibrated against a Pitot-static tube pair, located within the mid height of the tunnel and about 5cm apart. A CCD camera fitted with a macro lens is used to check that the wire is parallel to the wall and to make a first estimate of the distance of the wire from the wall. The counted number of pixels between the wire and its image on the tunnel surface is converted into distance using a conversion ratio from a calibration of the optical system. The uncertainty in the wall distance is estimated to be $\pm 5\mu\text{m}$.

Following calibration, the wire is positioned at the first measuring point, based on an initial estimate from the optical system. The measured mean velocity at that level is used to find a more accurate wall distance assuming that the Reichardt [9] formulation for the mean velocity profile is valid within the viscous sub-layer. No further adjustment is made to the wall distance. The validity of the measuring technique is verified by comparing the near wall data with other reliable and independent data. The friction velocity is obtained using the Clauser chart technique, with $\kappa = 0.41$ and $A = 5.0$, where A is the smooth wall constant.

Hot-wire signals were sampled on-line with an IBM compatible personal computer, using a Microstar 16 bit data acquisition board model DAP3000a/21. Turbulence intensity measurements were taken in burst of 8000 samples of 200Hz. Four bursts were sufficient to obtain converged results to within 1%. The u-spectra were measured with calibrated normal wires. The signals were sampled at three sampling rates of 500, 5,000 and 50,000Hz and

low-pass filtered at 200, 2,000 and 20,000Hz respectively, using Frequency Devices filter model LP00. A fast Fourier transform algorithm was used to calculate digitally the power spectral density of the signal. The three spectra files were then matched, joined and smoothed to form a single spectrum file. Taylor's hypothesis of frozen turbulence was used to transform the spectral argument from the frequency domain, f , to the wave number domain k_1 , such that

$$k_1 = \frac{2\pi f}{U_c}, \quad (2)$$

where U_c is the local mean convection velocity, which is assumed to be equal to the local mean velocity. The spectra were normalized such that

$$\int_0^\infty \Phi_{11}[k_1] dk_1 = \overline{u^2}, \quad (3)$$

where $\Phi_{11}[k_1]$ is the power spectral density per unit stream-wise wave-number k_1 .

Results and Discussion

Preliminary measurements

Preliminary measurements were carried out at low Reynolds number to check and validate the current measuring technique and instrumentation. The measuring station is located at 1.5m downstream the tripping device. The reference freestream velocity is 10m/s , which produced a boundary layer of thickness $\delta_c = 38.6\text{mm}$ and $R_\theta = 2600$. The mean flow velocity profile and streamwise turbulence intensity profiles, normalised with inner flow variables, are shown in figure 2 and compared with the LDA data of DeGraaff & Eaton [2] at $R_\theta = 2900$. Good agreement is observed down to the first measuring point. The difference in the mean flow in the outer flow region is related to the slight difference in R_θ . The lack of agreement of turbulence intensity profiles in the outer flow region is not known. These measurements show that the current approach for positioning, calibrating and measuring the wall distance for the wires is valid and accurate and can be used with confidence at other measuring stations.

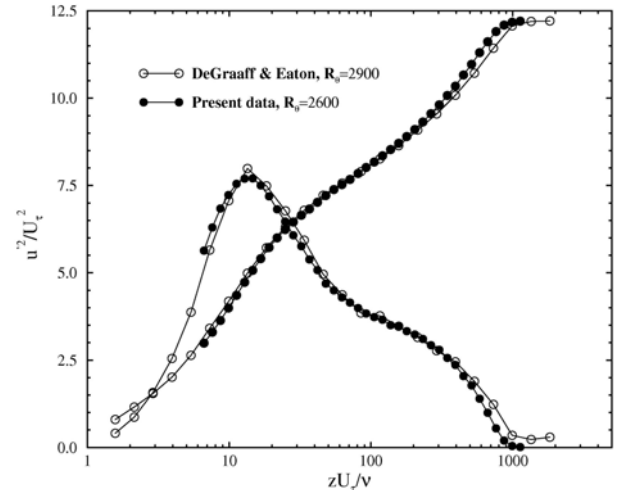


Figure 2: Comparison between normal hot-wire and LDA at low Reynolds number, with inner flow scaling. The vertical-axis label and values are shown for turbulence intensity profiles only. Mean flow velocity profile values are scaled down by 2.

Mean flow velocity profiles

Measurements for matched Reynolds number were carried out at three stations along the symmetry plane of the tunnel. The

Reynolds number, R_0 , for the most downstream station at the lowest reference velocity is approximately 20,000. This value is kept constant within $\pm 0.7\%$ for the other two measuring stations. Mean flow parameters used for scaling the measurements are shown in Table 1.

	21.7	13.7	8.7
X (m)	21.7	13.7	8.7
δ_c (mm)	335.9	214.9	140.5
v/U_τ (μm)	46.8	28.6	18.5
U_∞ (m/s)	10.0	16.0	24.0
η (μm)*	118.4	72.4	46.8
l/η	4.2 & 7.6	8.3 & 13.8	12.8 & 21.8
l^+	10.9 & 19.2	21.1 & 34.9	32.4 & 53.4

*Estimated value of η at $z^+=100$.

Mean flow velocity profiles, scaled with inner flow variables, are shown in figure 3. Profiles show complete collapse throughout the whole layer. The DNS data of Spalart [11], for $R_0=1410$ is also shown. The agreement is excellent for $z^+ < 100$, $z^+ \equiv z U_\tau / \nu$. The difference of approximately 1% between Pitot-static tube measurements and hot-wire measurements is acceptable. This difference can be reduced by applying a turbulence correction to the data collected by the impact pressure probe. This has not been done to the Pitot tube data shown in figure 3. The turbulence correction is more important for increasing Reynolds number. Developing similarity laws without such corrections may lead to wrong conclusions. Normal hot-wire data, plotted in the velocity defect form show complete collapse throughout the boundary layer. This result is consistent with the mean flow measurements using Pitot-static tube in the same wind tunnel (see Hafez *et al.* [4]). The velocity defect similarity arguments proposed by Castillo *et al.* [1] are not supported by our finding. They argued that for a certain tripping device type and location, different reference free stream velocities will yield different velocity defect curves.

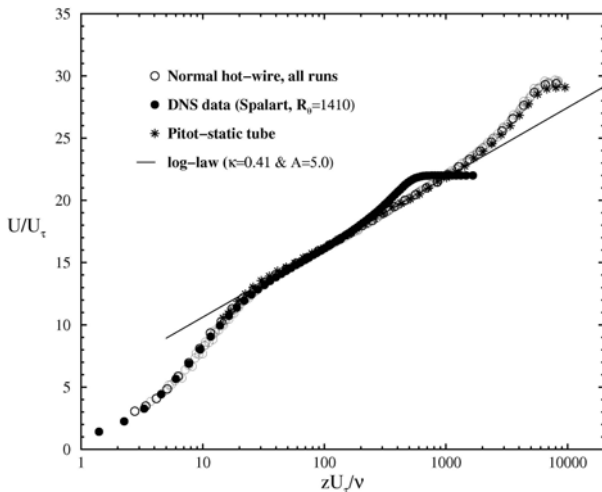


Figure 3: Mean flow velocity profiles, inner flow scaling.

Streamwise turbulence intensity

Figures 4 and 5 show the streamwise turbulence intensity profiles taken at the three measuring stations with different wire lengths. The spatial resolution effects can be seen up to relatively high z^+ values of about 300. Moving towards the wall the differences between profiles become more significant and account for about 40% of the near-wall maximum peak values. The 10m/s case represents the most resolved measurement in our study (with l^+ of 11 and 19) and differences are limited to small values of $z^+ < 15$. This result is in agreement with the finding of

Ligrani & Bradshaw [6], but not with Hites [5]. The data of Hites at $R_0=19,000$ (as discussed earlier), were measured with wires of length l^+ of 6 and 31. Hites' data gave a peak value of about 7.3 at about $z^+=15$, and roughly constant value of 5.8 for $70 < z^+ < 700$. These values agree well with the present measurements at 24m/s and wire length l^+ of 32.4. This indicates that Hites' data with the short wire, $l^+=6$, may represent unresolved flow.

The wire length is found to have a major effect on the present results. However, close examination reveals differences between wires of similar l^+ , but different freestream velocity. The increase in freestream velocity appears to adversely affect the measurements leading to further attenuated results. The reason for this could be an increase in end conduction heat loss.

An interesting feature of the plots is the continued attenuation of the measured turbulence intensity for z^+ up to about 300. The highly attenuated profile, for $l^+=53$, can be seen to have double peaks, one close to the wall and the other at z^+ of about 300. This behaviour represents loss of turbulent energy over a large portion of the boundary layer. Similar trends have been observed in boundary layer flows by Fernholz & Finley [3] and more recently by Morrison *et al.* [7], and is probably due to the lack of spatial resolution.

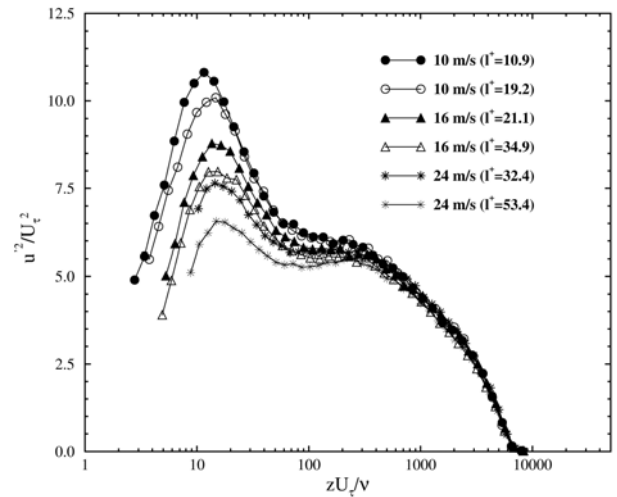


Figure 4: Streamwise turbulence intensity profiles, inner flow scaling.

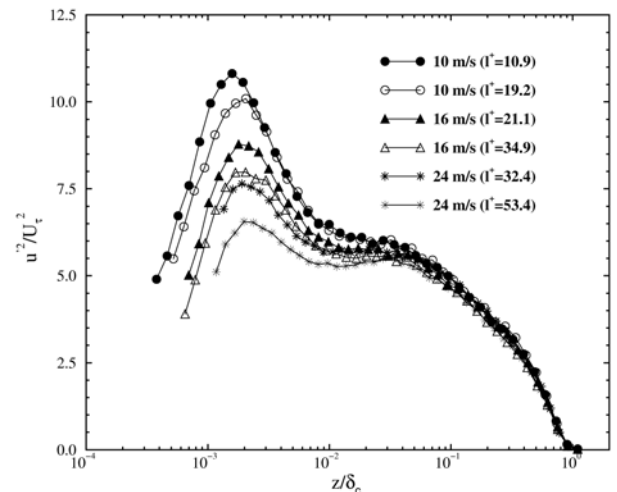


Figure 5: Streamwise turbulence intensity profiles, outer flow scaling.

Spectra

In this paper spectra measurements for the streamwise turbulence intensity are presented at $z^+=100$, for $R_0=20,000$ and for different freestream velocities, and hence different l^+ . Measured spectra are presented in the outer flow scaling and its respective pre-multiplied form in figures 6 and 7, respectively. According to

Perry *et al.* [8], within the turbulent wall region, spectra with outer and inner flow scaling should collapse onto the -1 or inverse power law envelope. Since the present measurements are collected at the same value of z^+ and the same R_θ , they should follow the same spectrum, provided that the flow is adequately resolved.

The plots demonstrate qualitatively the effect of using long wires. Figure 6 shows the peeling off trend for increasing wire length. Figure 7 shows the effect on the inverse power law plateau in the premultiplied spectra. These results highlight the difficulty of measuring highly resolved spectra.

The lack of spatial resolution could be a major factor and as pointed out by Smits & Dussauge [10]: “For long wires, the effects, spatial resolution, are more severe and begin at lower wave numbers”.

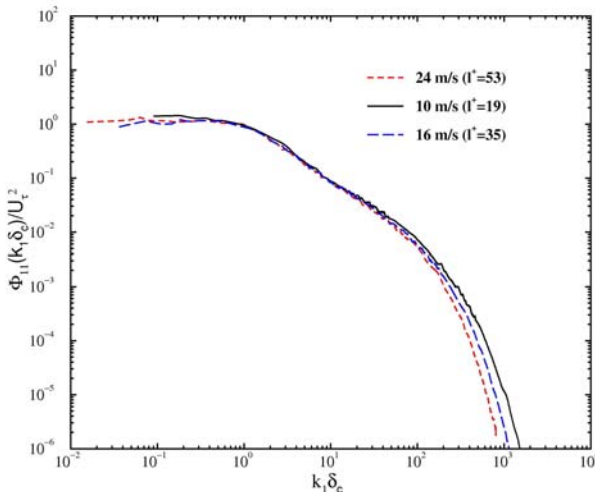


Figure 6: u-spectra with outer flow scaling at $z^+=100$.

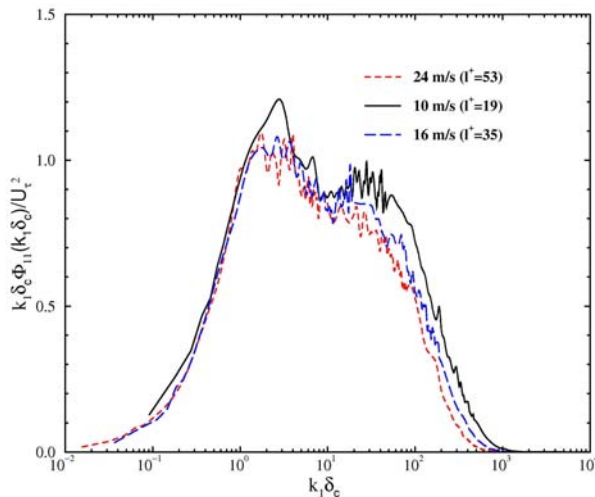


Figure 7: Pre-multiplied u-spectra with outer flow scaling at $z^+=100$.

Conclusions

An experimental study of the effects of spatial resolution on turbulent boundary layers measurements at high Reynolds number has been presented. Measurements are carried out at $R_\theta=20,000$ with wires non-dimensional length, l^+ , ranging from 11–54.

Mean flow measurements showed that turbulence correction might improve agreement between Pitot-tube and hotwire measurements. The mean flow velocity defect profiles showed independence of relevant freestream velocity. This finding is consistent with previous measurements in the same facility using Pitot-static tube but do not support the mean flow velocity defect similarity laws proposed by Castillo *et al.* [1].

Ligrani & Bradshaw [6] criterion for selecting hotwires suitable for resolving turbulent flows is found to be adequate, provided that flow velocity is low. However, with increasing bulk velocity even for properly selected wires may have further attenuations. This may be a result of increasing end conduction loss which reduces the effective length of the wire. The presence of a second peak, away from the wall in the turbulence intensity profiles, observed at high Reynolds number flows, may be due lack of spatial resolution.

Spectra measurements have shown that spatial resolution may be a serious problem, even with the limited range of l^+ employed in this study.

Acknowledgments

SH, MSC and MBJ wish to acknowledge the financial assistance of the Australian Research Council. IM would like to acknowledge support from NSF and the Packard Foundation.

References

- [1] Castillo, L., Seo, J., Hangan, H. and Johansson, T.G., Smooth and rough turbulent boundary layers at high Reynolds number. *Exp. Fluids*, **36**, 2004, 759-774.
- [2] DeGraaff, D.B. & Eaton, J.K., Reynolds-number scaling of the flat-plate turbulent boundary layer, *J. Fluid Mech.*, **422**, 2000, 319-346.
- [3] Fernholz, H.H. & Finley, P.J., The incompressible zero-pressure-gradient turbulent boundary layers: An assessment of the data. *Prog. Aerospace. Sci.*, **32**, 1996, 245-311.
- [4] Hafez, S., Jones, M.B. and Chong, M.S., The zero pressure gradient turbulent boundary layer and its approach to equilibrium, Proc. of the 10th AFMC, Peradeniya, Sri Lanka, 2004.
- [5] Hites, M.H., Scaling of High-Reynolds number Turbulent Boundary Layers in the National Diagnostic Facility, Ph.D. thesis, Illinois Institute of Technology, 1997.
- [6] Ligrani, P.M. & Bradshaw, P., Spatial resolution and measurement of turbulence in the viscous sublayer using subminiature hot-wire probes, *Expt. Fluids*, **5**, 1987, 407-417.
- [7] Morrison, J.F., McKeon, B.J., Jiang, W. and Smits, A.J., Scaling of the streamwise velocity component in turbulent pipe flow, *J. Fluid Mech.*, **508**, 2004, 99-131.
- [8] Perry, A.E., Henbest, S. and Chong, M.S. A theoretical and experimental study of wall turbulence. *J. Fluid Mech.*, **165**, 1986, 163-199.
- [9] Reichardt, H, Volständige darstellung de turbulenten geschwindigkeitsverteilung in glatten leitungen. *Zeitschrift für Angewandte mathematik und mechanik*, **31**, 1951, 208.
- [10] Smits, A.J. & Dussauge, J.P., *Turbulent Shear Layers in Supersonic Flow*. AIP Press, 1996.
- [11] Spalart, P.R., Direct simulation of a turbulent boundary layer up to $R_\theta=1410$, *J. Fluid Mech.*, **187**, 1988, 61-98.